Accepted Manuscript

Effect of hydrogen bonding on the infrared absorption intensity of OH stretch vibrations
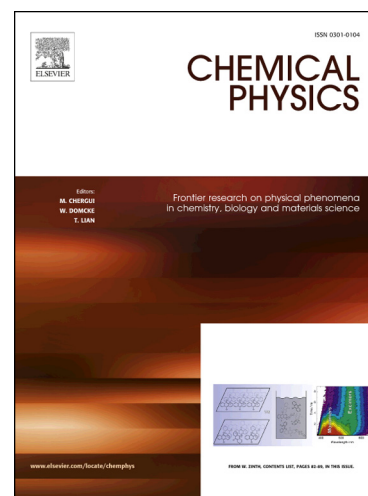
Bijyalaxmi Athokpam, Sai G. Ramesh, Ross H. McKenzie

CHEMICAL PHYSICS

ISSN 0301-0104

Editors:
M. CHERGUI
W. DOMCKE
T. LIAN

Frontier research on physical phenomena in chemistry, biology and materials science

www.elsevier.com/locate/chemphys

FROM M. ZINTH, CONTENTS LIST, PAGES 82-89, IN THIS ISSUE.

Effect of hydrogen bonding on the infrared absorption intensity of OH stretch vibrations

Bijyalaxmi Athokpam[a], Sai G. Ramesh[a], Ross H. McKenzie[b]

[a]*Department of Inorganic and Physical Chemistry, Indian Institute of Science, Bangalore 560 012, India*
[b]*School of Mathematics and Physics, University of Queensland, Brisbane 4072, Australia*

Abstract

We consider how the infrared intensity of a hydrogen-bonded OH stretch varies from weak to strong H-bonds using a theoretical model. We obtain trends for the fundamental and overtone transition intensities as a function of the donor-acceptor distance, a common measure of H-bond strength. Building upon our earlier work using a two-diabatic state model, we introduce a Mecke function-based dipole moment for the H-bond and calculate transition moments using one-dimensional vibrational eigenstates along the H-atom transfer coordinate. The fundamental intensity is found to be over 20-fold enhanced for strong H-bonds, where non-Condon effects are significant. We analyse isotope effects, including the secondary geometric isotope effect. The first overtone intensity varies non-monotonically with H-bond strength; suppression occurs for weak bonds but strong enhancements are possible for strong H-bonds. We also study how these trends are affected by Mecke parameter variations. For a few specific dimers, we compare our results with earlier works.

1. Introduction

A well-known signature of the O-H$\cdots$O hydrogen (H) bond, in addition to the red-shift of the O-H stretch frequency, is a strong increase in the absorption intensity of the infrared band of this mode [1, 2]. References [3, 4, 5, 6, 7, 8, 9, 10, 11] are but a subset of the many works that have previously addressed this effect. The work by Iogansen [7] is particular in that it established an empirical relation between the hydrogen bonding energy and the intensity of the infra-red absorption of the O-H stretching mode for a wide range of compounds:

$$\Delta H = -12.2(A^{1/2} - A_0^{1/2}), \tag{1}$$

Email addresses: `sai.ramesh@ipc.iisc.ernet.in` (Sai G. Ramesh),
`r.mckenzie@uq.edu.au` (Ross H. McKenzie)
URL: `condensedconcepts.blogspot.com` (Ross H. McKenzie)

where ΔH is the enthalpy (kJ/mol) of H-bond formation and A and A_0 are the intensities (in units of 10^4 cm mmol^{-1}=100 km/mol) of O-H stretch in the presence and absence of the H-bond respectively. This holds for energies varying by a factor of 200 (between about 0.3 and 60 kJ/mol), thus spanning from weak to strong H-bonds. Ratajczak, Orville-Thomas, and Rao [12] considered a theoretical basis for the empirical relation given in equation (1) using Mulliken's charge transfer theory. Rozenberg [13] recently suggested a relation between H-bond enthalpy and electron density at the bond-critical point from atoms-in-molecules theory, and thereby an indirect linear relation between intensity and electron density. Fillaux [6], though primarily concerned with the theory of H-bond band shapes, conjectured a non-monotonic relationship between intensity A and the donor-acceptor distance R, with a maximum around $R \simeq 2.6$ Å.

Bratos et al. reviewed experiments describing the variation of the intensity enhancement with the strength of the H-bond in liquids, which are viewed as static disordered media [5]. For weak H-bonds ($R > 2.8$Å) they find enhancement in the range of about 5 to 10. For medium strong H-bonds ($R \sim 2.6 - 2.8$ Å), it is enhanced by 10 to 15, while for strong H-bonds it becomes as large as about 30. For strong symmetrical H-bonds ($R < 2.6$ Å), the enhancement of A decreases by about 10 when R decreases from 2.5 to 2.45 Å, consistent with a non-monotonic dependence on R. However, estimating the intensity accurately is difficult due to the broad spectra.

H/D isotope substitution causes a suppression in the O-H stretch intensity. For free O-H bonds, one anticipates a decrease by a factor of two in the harmonic picture. The suppression changes with H-bond strength as well. For instance, Bratos et al. [5] state that $A_H/A_D \simeq 2$ for weak H-bonds, which gets enhanced by ~ 2.6 for medium bonds and $\sim 3-5$ for strong H-bonds (see note in Ref. [5]).

In contrast to the fundamental transition, a number of studies have reported that the intensity of the first overtone of the O-H stretch shows a pronounced suppression upon H-bonding [14, 10, 11, 9]. Indeed, eighty years ago failure to observe a OH stretching overtone was correlated with the presence of an H-bond.[15] Di Paolo et al. [14] explained this in terms of a balance between mechanical and electrical anharmonicity. Suhm and co-workers' studies of a range of alcohol dimers [10, 11] report fundamental-to-overtone intensity ratios in the range of 300 to 1000 for the H-bonded OH stretches, compared to about 10 for the monomeric OH. For diols, Howard et al. [9] found that the suppression increases for the donor O-H with H-bond strength from ethane- (~ 15) to propane- (~ 83) to butanediol (~ 500). The acceptor O-H has a smaller value of about 7. We parenthetically note that the study of overtones is interesting in its own right: Heller [16] pointed out that overtone excitation is a purely quantum effect, associated with dynamical tunneling, just like reflection above a potential barrier. Lehmann and Smith [17] and Medvedev [18] considered the factors that influence overtone intensity of hydrogen stretches in simple molecules. They showed that the intensity of the $0 \rightarrow n$, $n \geq 2$, overtones is sensitive to the shape of the (inner) repulsive wall of the stretch potential, i.e. the classically forbidden region. Medvedev [18] has also noted that, though the electrical anharmonicity affects the intensity by upto an order of magnitude

2

relative to when a linear dipole is used, it does not affect the general trend of several orders of magnitude drop in the overtone intensities with n.

In this paper we study the intensity variation of the O-H stretch transition with H-bond strength using a simple one-dimensional two-state diabatic model potential. Using this model, our prior works have discussed vibrational frequencies along the OH stretch coordinate, H-atom position, primary and secondary (geometric) isotope effects, as well as isotopic fractionation [19, 20, 21]. The present work adds to the model a dipole moment function, based on the Mecke form [22], along the OH stretch coordinate in order to compute the intensities. Section 2 briefly describes the diabatic model, the dipole moment function we use, the Condon approximation, and some of the computational details. Section 3 presents results for the O-H fundamental intensity variation, isotope effect on the fundamental intensity, the first overtone intensity variation, and the effect of modifying the dipole function shape. In Section 4 we give a detailed comparison of our results with previous theoretical and experimental works. We offer some remarks in the concluding section.

2. Computation of the infrared intensity

The intensity of a vibrational transition $j \leftarrow i$ is experimentally obtained as the integral molar absorption coefficient over the corresponding spectral band, [23, 7]

$$A_{ji} = -\frac{1}{c\,\ell} \int \ln T(\tilde{\nu}) d\tilde{\nu}. \tag{2}$$

where T is the transmittance, c in the concentration, and ℓ is the path length. The unit for A_{ji} is km/mol. Time-dependent perturbation theory yields the theoretical expression for the intensity as [23]

$$A_{ji} = \frac{2\pi^2}{3\epsilon_0 hc} \tilde{\nu}_{ji} |\mu_{ji}|^2, \tag{3}$$

where the transition dipole matrix element

$$\mu_{ji} = \int dr \phi_j^*(r) \mu_g(r) \phi_i(r) \tag{4}$$

where $\nu_{ji} = E_j - E_i$ and $\phi_i(r)$ is a vibrational wave function and r denotes the nuclear co-ordinates. Here $\tilde{\nu}_{ji}$ is in cm^{-1}, μ is in Debye, and the units of A_{ji} are km/mol. In the present work on O-H$\cdots$O H-bond intensities, we focus on the hydrogen atom motion along the O-O axis. We therefore consider the wavefunctions and the dipole moment along this line alone.

In order to have a sense of the magnitude of A, we note that simple alcohol monomers are reported to have experimental and theoretical gas phase fundamental intensities in the range of about 25 km/mol [24, 25, 26]. The corresponding gas phase dimers show an intensity enhancement of about an order of magnitude [9, 10, 26]. Several studies on the $(H_2O)_2$ dimer have shown signficant

3

enhancement with respect to the monomer [27, 28, 29, 30, 31, 32, 33, 34, 35]: the intensities are about 45 and 140 km/mol for the monomer (asymmetric stretch) and dimer, respectively.

The linearized dipole approximation is often applied to Eq. (4), where only the first derivative of the dipole function is used in the intensity expression:

$$\mu_{ji} \simeq \mu_{ji}^C \equiv \frac{\partial \mu_g(r_{eq})}{\partial r} r_{ji}, \qquad (5)$$

where r_{ji} is the matrix element of the OH coordinate (r) between the jth and ith states, and r_{eq} is the equilibrium O-H bond length (i.e. the value of r at which the potential energy is a minimum along the O-H stretch). Some authors refer to this as the *Condon approximation* following the introduction by Condon [36] to the treatment of electronic transitions. We shall follow this nomenclature. Deviations from the Condon approximation are also known as electrical anharmonicity.

The Condon approximation leads to several further analyses. (1) There are two distinct physical mechanisms whereby H-bonding can increase the intensity. The first is by increasing the dipole derivative. The second is by increasing the position matrix element, which will be related to the amount of zero-point motion. (2) If the nuclear wave functions are harmonic, then the only vibrational transition with non-zero intensity is that of the fundamental (i.e. from the ground state $i = 0$ to the first vibrational excited state, $i = 1$). There are no overtones, i.e. higher harmonics. This is known as the *double harmonic approximation*. (The first is the Condon approximation). In reality, all potential energy surfaces are anharmonic and so this leads to the presence of weak overtones in IR spectra. Their intensity can be used to estimate the amount of anharmonicity, both in the potential and the dipole moment surface (i.e. deviations from Condon). In the harmonic approximation, $|r_{01}|^2 \sim \hbar/(m\omega) \propto 1/\sqrt{m}$, where ω is the harmonic frequency of the oscillator. This gives a limiting value for the isotope effect on the fundamental intensity: $A_H/A_D = 2$. (3) The Thomas-Reiche-Kuhn (TRK) sum rule [37] relates the oscillator strengths of the ground-to-excited-state transitions:

$$\sum_j (E_j - E_0)|r_{j0}|^2 = \frac{\hbar^2}{2m}. \qquad (6)$$

E_j is the energy of the jth vibrational state and m is the reduced mass of the oscillator. This is true for any potential. In the Condon approximation (Eq. (5)), the terms in the summation differ from the intensity (Eq. 3) by a common pre-factor the dipole derivative. Generally, the sum will be dominated by the fundamental.

The intensities of overtones involve contributions from both electrical and mechanical anharmonicities. Early work by di Paolo et al. [14] showed that, for a Morse oscillator with second-order dipole expansions, the two anharmonicities have cancelling influences for the first overtone's intensity while being additive for the fundamental. Ref. [10] found that the relative signs of the dipole moment

first and second derivatives for H-bonded OH of 2,2,2-trifluoroethanol dimer to be in agreement with this notion.

Recent works have quantified the effect of the two anharmonicities on the fundamental and overtone intensities of infrared lines for simple molecules. For example, Vazquez and Stanton [38] studied H_2O and HFCO, while Banik and Durga Prasad [39] studied H_2O and H_2CO. For these simple isolated molecules the effect of the anharmonicities on the intensity of the fundamental is typically only a few per cent. For molecules that have weak fundamentals (due to small dipole first derivatives) and stronger overtones, the anharmonicities would play a greater role.

Whether the assumption of slow variation of the dipole moment over the relevant length scale of the oscillator wave functions is applicable for H-bonded complexes, at various H-bond strengths, is a relevant question. To the extent that it is valid, the other contribution to the intensity is the mechanical anharmonicity. This increases as H-bonding strengthens, which results in an increase in intensity as well. However, there are significant cases of non-Condon effects. Schmidt, Corcelli, and Skinner [40] found that for the OH stretch in liquid water one needs to take into account the dependence of the dipole moment on the nuclear co-ordinates of the surrounding water molecules. McCoy et al. [41] argued that there were large non-Condon effects in $H_3O^+ \cdot X_3$ (X = Ar, N_2, CH_4, H_2O) complexes and suggested this is relevant to the intensity of the 'association band' seen in the vibrational spectrum of liquid water.

2.1. Diabatic state model for H-bonding

In this work, we use the two-state diabatic state model for linear symmetric O-H$\cdots$O H-bonds from recent work by McKenzie [19]. It was shown in subsequent work [20, 21] that it affords a quantitative description of the correlations observed [42] between the OO distance (R) and OH bond lengths (r), the frequencies of OH vibrations (both stretch and bend), and H/D isotope effects for a diverse range of chemical compounds [20, 21]. We use the same notation and parameters as in Ref. [20].

For a O-H$\cdots$O complex, the Hamiltonian with respect to the diabatic states, $|$O-H$\cdots$O$\rangle$ and $|$O$\cdots$H-O$\rangle$, is given as

$$H = \begin{pmatrix} V(r) & \Delta(R) \\ \Delta(R) & V(R-r) + V_o \end{pmatrix} \tag{7}$$

The coordinates r and R are the OH and OO distances, respectively, and r_0 is the equilibrium free OH distance of 0.96 Å. $V(r)$ is Morse potential with a depth (D) of 120 kcal/mol, an exponential parameter (a) of 2.2 Å^{-1}, corresponding to a harmonic frequency of 3600 cm^{-1}. Its arguments r and $R-r$ in Eq. (10) point to the O-H$\cdots$O and O$\cdots$H-O diabats, respectively. V_o is a vertical offset. In this work, we consider both symmetric and asymmetric cases; more details are at the end of this subsection. The coupling between the diabats is given as $\Delta(R) = \Delta_1 \exp(-b(R - R_1)$, with $\Delta_1 = 48$ kcal/mol, $b = a$, and $R_1 = 2r_0 + 1/a \approx 2.37$ Å. We note that this is the abbreviated form of the coupling:

5

The full form contains an angular dependence on the two HOO angles as well [19].

We treat the donor-acceptor distance R as a control parameter. The electronic ground state for the above Hamiltonian is given as

$$|\Psi_g(r|R)\rangle = -\sin\theta(r|R)\,|\text{O-H}\cdots\text{O}\rangle + \cos\theta(r|R)\,|\text{O}\cdots\text{H-O}\rangle \qquad (8)$$

where the angle is given by

$$\tan 2\theta(r|R) = \frac{2\Delta(R)}{V(r) - V(R-r) - V_o}. \qquad (9)$$

We note that this form for the ground state of the electronic wavefunction allows for the charge transfer character of a H-bond, as emphasized by Thompson and Hynes [43]. The potential curve corresponding to this state is

$$\epsilon_-(r, R) = \tfrac{1}{2}\left[V(r) + V(R-r) + V_o\right]$$
$$- \tfrac{1}{2}\left[(V(r) - V(R-r) - V_o)^2 + 4\Delta(R)^2\right]^{\frac{1}{2}}. \qquad (10)$$

For $V_o = 0$, this yields a symmetric double well. This is a suitable choice for strong bonds, since the H atom is essentially shared by the donor and acceptor. In other words, the respective pK_a's are about the same [42]. However, for weak H-bonds, a sizeable V_o is more appropriate. In this work, we consider $V_o = 0$ at all R, and $V_o = 50$ kcal/mol for $R \geq 2.7$ Å. In the latter case, we discuss the variability of the results with asymmetry.

2.2. Vibrational eigenstates

The vibrational eigenstates used in this work to compute infrared intensities are the one-dimensional vibrational eigensolutions for a H/D atom on $\epsilon_-(r|R)$. They are calculated using sinc-DVR functions [44]. For the $V_o = 0$ case, the potential is a symmetric double-well. Hence, the solutions are labelled $\phi_{n\pm}$ or $n^\pm$, where $\pm$ indicates symmetric and antisymmetric tunnel-split doublets. Of course, such a label is truly relevant only if the energy levels are well-below the barrier height. However, we use these labels at all R; see Ref. [20] for further details. For the asymmetric cases, we simply drop the $\pm$ subscript.

Of primary interest in this work are the ground ($\phi_{0\pm}$ or ϕ_0), first excited ($\phi_{1\pm}$ or ϕ_1), and second excited ($\phi_{2\pm}$ or ϕ_2) states. Transitions between these states define the fundamentals and overtones we analyse.

When H is replaced with D, a secondary geometric isotope effect (SGIE) is observed, wherein the O-O distance changes [45, 46, 47]. This is purely a quantum effect based on the vibrational zero-point energy gradients. Within our diabatic model, as the H-bond strengthens from $R = 3.0$ Å to about $R = 2.45$ Å, deuteration leads to a progressive increase in the O-O equilibrium distance of up to about 0.04 Å. Though small in magnitude, it was found to yield significant H/D frequency effects [20]. This is because changing R changes the shape of the OH stretch potential, and small changes in R are particularly significant in

the regime of low-barrier H-bonds where the energy barrier is comparable to the OH stretch zero point energy. For $R \lesssim 2.4$ Å, the direction of the trend is found to be reversed. In analysing the role of SGIE on the intensities, the eigenenergies and wavefunctions for deuterium are computed at two distances, namely without and with the model-estimated O-O distance change. This is carried out only for the symmetric case, $V_o = 0$.

2.3. Dipole moment function for an H-bonded complex

For the two diabats, the O-H dipole moments point in opposite directions. For a symmetric H-bond, it is then evident that the ground adiabatic state dipole moment function, $\mu_g(r|R)$, would be antisymmetric. To generate such a dipole function, we assume the following form of the *diabatic* dipole function:

$$\hat{\mu}_d = \begin{pmatrix} \mu_0(r) & 0 \\ 0 & -\mu_0(R-r) \end{pmatrix}, \tag{11}$$

where $\mu_0(r)$ is a suitable, common form for the dipole moment of both diabats, and the explicit sign indicates the dipole direction. This is the Mulliken-Hush approach [48] where there is no cross term in the diabatic representation of the dipole moment. We also assume that the choice of common form of $\mu_o(r)$ for both diabats holds for asymmetric H-bonds as well. In that case it is an approximation.

This leads to the definition of the adiabatic dipole surface $\mu_g(r)$ as

$$\begin{aligned} \mu_g(r|R) &= \langle \Psi_g | \hat{\mu}_d | \Psi_g \rangle \\ &= \sin^2 \theta(r|R)\mu_0(r) - \cos^2 \theta(r|R)\mu_0(R-r) \\ &= \mu_0(r) - \cos^2 \theta(r|R) \left\{ \mu_0(r) + \mu_0(R-r) \right\}, \end{aligned} \tag{12}$$

where from (9)

$$2\cos^2 \theta(r|R) = 1 + \frac{V(r) - V(R-r) - V_o}{\sqrt{[V(r) - V(R-r) - V_o]^2 + 4\Delta^2}}. \tag{13}$$

It remains to choose a form for $\mu_0(r)$, which we discuss in the next subsection.

The *Condon approximation* (Eq. (5)) for $\mu_g(r)$ involves the evaluation of its derivative at $r_{eq}(R)$, which is the minimum of the adiabatic potential $\epsilon_-(r|R)$ at different R. The approximation would be valid to the extent that this shape of $\mu_g(r)$ is approximately linear in a sufficiently wide interval about r_{eq}. In Section 3.2, we will compare the dipole moment function $\mu_g(r)$ with the wavefunction shapes at different R to determine if this is so.

We note the selection rules for the fundamental and overtone transitions. Since $\mu_g(r)$ is antisymmetric in r for all R, the allowed transitions involve a change in the symmetry of the vibrational wavefunction, i.e., a change in parity. We focus on three transitions: $1^+ \leftarrow 0^-$, $1^- \leftarrow 0^+$, and $2^+ \leftarrow 0^-$. In section 3.1, we discuss the possible identification of these transitions with the fundamental and first overtone. See also the discussion in Sec. V of Ref. [20].

7

2.4. Dipole moment function for diabatic states

In choosing a form of the diabatic dipole moment, we make a bond dipole approximation. We note that molecular dipole moments are not always oriented along bonds. However, our diabatic model (Sec. 2.1) treats the donor and acceptor as unified atoms. In keeping with this, the present one-dimensional treatment only affords a dipole moment along the O-O axis. We therefore do not use a vector notation for the dipole moment throughout this work.

A simple analytical form of a bond dipole moment function is that due to Mecke [22]:

$$\mu_0(r) = \mu^* r^m \exp(-r/r^*). \tag{14}$$

This three-parameter function has the desired limits in that it vanishes for small and large r. It has the maximum magnitude at $r = mr^*$. Usually, m is fixed to be 1. The Mecke form has been used in both theoretical and experimental studies in the literature [49, 50, 51, 52, 25, 53, 54, 55, 56]. It has the significant advantage that although it depends on just a few parameters it can be used to give a quantitative description of the intensity of many overtones. For example, for OH stretch vibrations, Phillips and coworkers have used the Mecke form to describe the intensities of up to the fourth overtone of vapour phase alcohols, including methanol, ethanol, and isopropanol, as well as acetic and nitric acid [25, 54]. The intensities of the CH overtones for naphthalene have been studied by Schek et $al.$ [49] using this dipole form, while those in haloforms have been extensively studied by Quack and coworkers [51]. Lin et $al.$ have analysed SiH_4 and GeH_4 local mode overtone intensities using a local bond dipole model, for which they fit ab $initio$ dipole moments to Mecke forms (yielding $m \simeq 0.7$ and a maximum near the equilibrium bond length for both molecules) [53]. Lemus and coworkers have explored the continuum effects in coupled Morse oscillators using a Mecke form for associated dipoles [56].

In the context of O-H bonds, it has been argued that the Mecke form might not be suitable for monomeric species [55, 57], and that Taylor expansions up to a suitable order appear better. However, the present work aims at exploring trends for a wide range of H-bonds, from weak to strong, over a wide donor-acceptor range. On this account, we have chosen to retain the Mecke form for $\mu_0(r)$. We use the Lawton and Child [50] parameter values of $m = 1$, $\mu^* = 7.85$ D/Å, and $r^* = 0.6$ Å, originally given for the OH bond in water. All results in the sections 3.2-3.6 are with these parameters.

Two further aspects of our choice are of note. First, the dipole moment for the left and right diabats are assumed to arise from bond dipoles from the (donor) O-H and (acceptor) H-O alone; see Eq. (11) above. Second, the chosen $\mu_0(r)$ has a negative slope of -0.95 DÅ^{-1} at the equilibrium bond length, $r_0 = 0.96$ Å, since $r^* < r_0$. (Note: $\mu_0(r_0) = 1.52$ D, and $\mu_0''(r_0) = -1.06$ DÅ^{-2}.) This is a point of departure from ab $initio$ results for some OH monomers, where the first derivative is found to be positive [55]. In terms of the Mecke form, this means that r^*, the position of the maximum, occurs after r_0. It was also found that there was some variation of the position of the maximum with molecular identity. Motivated by this, we have also investigated r^* values that are smaller

8

and larger than r_0 and report our findings in Sec. 3.7. We note that r^* alone governs the shape of $\mu_0(r)$ (since m is held fixed at 1), and hence the results we present.

An alternative to using a simple analytical form for the dipole function is to perform *ab initio* calculations for specific molecular systems. However, it should be stressed that the results can vary significantly with basis set and level of theory used [57, 58, 59]. Furthermore, our goal is not to consider specific systems but rather to see if a simple model can capture trends observed across a wide range of systems.

3. Results
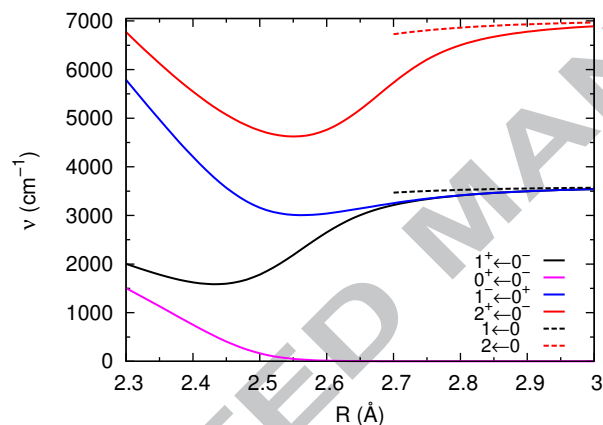
3.1. Frequency vs H-bond length (R)

Figure 1: Variation of different OH stretch transition frequencies with the donor acceptor R for symmetric and asymmetric H-bonds. *Solid lines, symmetric H-bonds:* The curves plotted are $1^+ \leftarrow 0^-$ (black), $1^- \leftarrow 0^+$ (blue), $2^+ \leftarrow 0^-$ (red), and $0^+ \leftarrow 0^-$ (magenta). For weak bonds ($R > 2.7$ Å) the black and red curves can be identified with fundamental and first overtone transitions respectively. The blue curve separates from the fundamental curve (solid black) only when the tunnel splitting becomes significant. For moderate bond strengths, the solid black curve has the lowest frequency in the experimentally relevant range (> 500 cm^{-1}) and so is identified as the fundamental. For strong bonds, there are large anharmonic effects and the nomenclature of fundamental and first overtone is not particularly meaningful. *Dashed lines, asymmetric H-bonds:* The $1 \leftarrow 0$ and $2 \leftarrow 0$ transition frequencies are plotted for $R \geq 2.7$ Å for an asymmetry (V_o) of 50 kcal/mol. The effective potential of the lower well is a little less anharmonic than for the symmetric case. Consequently, the transition frequencies are a little higher.

We begin with an analysis of the frequencies of different vibrational transitions as the H-bond strength changes for both symmetric and asymmetric cases. This is necessary, particular for the symmetric case, to clearly define what we mean by a *fundamental* and a *first overtone*, since there are significant anharmonic effects for strong bonds in the symmetric case. For weak symmetric or weak asymmetric H-bonds, the identification is straightforward.

The solid curves in Figure 1 are for the *symmetric* case. The frequency of the $1^+ \leftarrow 0^-$ transition frequency is seen to have a non-monotonic variation with R (black curve). It is progressively softened (red-shifted) as the H-bond strength changes from weak ($R \gtrsim 2.7$ Å) to moderately strong ($R \sim 2.5 - 2.6$ Å). In the latter region, the barrier height becomes comparable to the energy of the first few O-H vibrational states, and as a result the tunnel-splitting is significant. In the very strong H-bond region ($R < 2.45$ Å), the potential becomes roughly square-well like with a very low or no barrier, and all the vibrational states are energetically well separated. Hence the $1^+ \leftarrow 0^-$ curve turns upward. For moderate bond strengths, the black curve has the lowest frequency in the experimentally relevant range (> 500 cm^{-1}) and so is identified as the *fundamental*. The above discussion is based on Figure 3 in Ref. [20] which shows the different potentials and low-lying vibrational energies for $R =$ 2.3, 2.45, 2.5, 2.9 Å. See Refs. [60, 61, 62, 63] and the note in Ref. [64] for a brief list of systems with varying H-bond strengths.

Also shown in Figure 1 is the $2^+ \leftarrow 0^-$ transition frequency (red curve). This, too, has a non-monotonic dependence on R. For weak bonds, this can be identified as the *first overtone* as it has roughly twice the frequency of the fundamental. But it turns upward sooner compared to the fundamental since the energy of the 2^+ state, moves higher than the barrier before the 1^+ state does. In the moderate H-bond region, due to significant tunnel-splitting, the $1^- \leftarrow 0^+$ transition frequency (blue curve) clearly separates from the fundamental curve. The definition of the first overtone in this region becomes ambiguous due to the large anharmonicity of the potential. We discuss the intensities for each of these vibrational transitions in Section 3.6. Like the frequencies, they all have a non-monotonic dependence on R.

We also note that for strong bonds with $R \lesssim 2.5$ Å, the splitting of the 0^+ and 0^- levels becomes larger than 500 cm^{-1}, which is larger than the thermal energy, $k_B T$ at room temperature. This means that the population of the 0^- level will be reduced by a Boltzmann factor of order 0.1. In an experiment, there will be a corresponding reduction in the measured IR absorption intensity associated with transitions from this level. In order to highlight changes in the dipole matrix element, our plots do not take this thermal effect into account.

For the *asymmetric* case, the chosen V_o value shifts the right diabat in Eq. (7) above the energy of the Morse overtone level of the left (unshifted) diabat. The resulting ground state potential therefore has *single* and unambiguously identifiable ground, fundamental, and overtone levels. The corresponding wavefunctions are also largely localized on the left side. The fundamental and overtone transition frequencies as a function of R are plotted as red and blue dashed lines in Figure 1. The plots stop at 2.7 Å since we consider asymmetry only in the weak H-bonding regime. It is of note that the asymmetric fundamental is higher by 256 and 30 cm^{-1} compared to the symmetric case at 2.7 and 3.0 Å, respectively. The corresponding values for the overtone are 996 and 75 cm^{-1}. Both sets are consistently higher. A major part of these differences is due to the lower harmonic frequency of ground state potential minimum for the $V_o = 0$ case than for $V_o > 0$: The diabats are more mixed with decreasing asymmetry and

at shorter R in general. A smaller role is played by the effective anharmonicity of the ground state potential well, which reduces (to simply the anharmonicity of the Morse potential for the diabatic state) with increasing V_o.
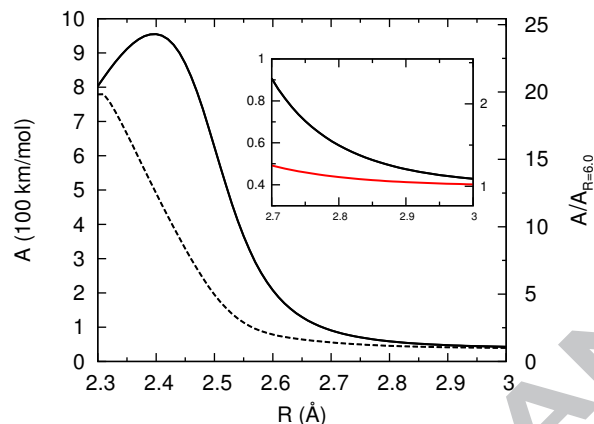
3.2. Intensity of the fundamental transition

Figure 2: Intensity of the $1^+ \leftarrow 0^-$ transition as a function of R. The left axis is intensity in (100 km/mol) units and the right axis is the intensity scaled with respect to its value for $R = 6.0$ Å (non-H-bonded OH). The solid line is the intensity obtained through the full matrix element, Eqn.(4), while the dashed line is obtained using the Condon approximation, eqn. (5). The inset is a blow-up of the curve, showing the relatively small intensity enhancements in the weak H-bond regime. Also shown in red in the inset is the trend when $V_o = 50$ kcal/mol.

For symmetric H-bonds, our calculation of the intensity of the $1^+ \leftarrow 0^-$ (fundamental) transition using eqn. (3) is shown by the solid line in Figure 2. The non-H-bonded OH intensity value (computed at $R = 6.0$ Å) is about 39 km/mol, which compares reasonably with the range of about $20 - 60$ km/mol reported for O-H stretches for a range of isolated molecules [24, 25, 26, 39]. The intensity enhancement relative to this value is a little over 2 in the weak H-bond region (see inset). As the curve enters the moderately strong H-bond region ($R \lesssim 2.6$ Å), it shows $\sim 5 - 10$ fold enhancement, reaching ~ 20 for strong H-bonds ($R \approx 2.4$ Å). This enhancement magnitude, though a little lesser, broadly agrees with experimental results summarized by Bratos et al. [5]

Figure 3 shows the contributions to the integrand in eqn. (4), viz. $\mu_g(r)$ and $\phi_{1+}\phi_{0-}(r)$, at different R, giving insight into the intensity enhancement with increased H-bond strength. These functions are both asymmetric about $r - R/2 = 0$ at all R. Hence it would suffice to consider only one vertical half of the plots. The first panel is for $R = 2.8$ Å. Here, $\mu_g(r)$ is mostly linear for a large O-H distance (r) range. The $\phi_{1+}\phi_{0-}$ product function amplitude is non-zero over roughly the same r range. Its positive and negative regions have only a small difference in areas, leading to significant cancellations in the total integral. However, this difference in areas is a little larger than that at $R = 3.0$ Å, where $\mu_g(r)$ is found to be even more clearly linear in the relevant r range. A

11

modest intensity enhancement at $R = 2.8$ Å compared to $R = 3.0$ Å is therefore anticipated, and borne out by the plot in Figure 2.

For moderate strength H-bonds ($R \sim 2.6$ Å, middle panel), $\mu_g(r)$ is seen to be more non-linear. This is a consequence of the shape of the mixing angle $\theta(r)$ with r [compare equations (8)) and (9)]; with decreasing R, it changes less abruptly along r between its diabatic limits of 0 and $\pi/2$. As a consequence, the charge transfer character changes more continuously as the proton moves from the donor to the acceptor. This is true for $\mu_g(r)$ as well. Returning to the wavefunction product, the $\phi_{1+}\phi_{0-}$ overlap function has more unequal positive and negative spread at $R = 2.6$ Å. This results in less cancellation compared to the case at $R = 2.8$ Å, resulting in a larger enhancement of intensity. All these effects becomes stronger still at $R = 2.4$ Å (bottom panel).

3.3. Break down of the Condon approximation

The dashed line in Figure 2 gives the intensity obtained using the Condon approximation (eqn.(4)). The required derivative of $\partial\mu_g(r)/\partial r$ was evaluated at the classical minimum of the double well for each R. In Figure 3, these are marked with blue plus signs. In the weak H-bond region (large R), the intensity calculated through this approximation is in agreement with the actual value. But as R decreases the approximation breaks down and is seen to underestimate the intensity. Figure 3 helps explain this Condon breakdown. For weak H-bonds, $\mu_g(r)$ is largely linear in the region where $\phi_{1+}\phi_{0-}$ has significant amplitude, as seen for $R = 2.8$ Å. Taking a constant dipole derivative for this case is reasonable. But as the H-bond strengthens, $\mu_g(r)$ is sufficiently non-linear for $R = 2.6$ Å, and even more so at $R = 2.4$ Å. For these cases, the $\phi_{1+}\phi_{0-}$ overlap curve becomes less localized, i.e., broader. This reflects the large zero-point motion due to the reduced frequency of the OH stretch and the increase in anharmonicity and tunneling. Hence, the actual intensity is more enhanced than that calculated with the Condon approximation.

3.4. Fundamental intensity for asymmetric H-bonds

We now discuss in detail the results for asymmetric H-bonds. The trend for R in the range 2.7-3.0 Å is shown as the red curve in the inset of Figure 2. Here, too, there is an enhancement in intensity with decreasing R, albeit smaller than that for the symmetric case. At $R = 2.7$ Å, it is about 1.25 times that for a free OH. This fraction varies slightly when the asymmetry is changed to 40 or 75 kcal/mol, the former (latter) leading to higher (lower) intensity. Insight into why these numbers are all lower than the symmetric case may be obtained from the work of di Paolo et al.[14] Translating their notation to ours, the fundamental intensity is proportional to $(\mu_g' - 5b\mu_g'')^2$, where the dipole derivatives are evaluated at the potential minimum, and b is the (dimensionless) ratio of the cubic anharmonicity to the harmonic frequency of the well. With $b < 0$ being the typical case, and μ_g' and μ_g'' having the same sign (which is true in our case as well), di Paolo et al. argued that the second term augments the first. Therefore, the potential and electrical anharmonicity enhance the

12

fundamental intensity. For our case, the symmetric case has both larger $|b|$ and larger μ_g'' than the asymmetric one at a given R. The underlying cause is the larger mixing of diabats in the symmetric versus asymmetric models, ultimately leading to the computed differences in intensities.

3.5. Isotope effect on the intensity of the $1^+ \leftarrow 0^-$ transition

Experiments show that the intensity of the fundamental transition of a H-bonded O-H stretch mode is suppressed upon substituting H by D.[5] The black curve of Figure 4 shows how H/D isotope substitution affects the intensity of the fundamental, as calculated for our symmetric H-bond model. (We limit the analysis to the symmetric case since the effects discussed below are more important in the medium and strong H-bonds.) The A_H/A_D ratio shows a non-monotonic dependence on R. In the weak H-bond region, the ratio is almost unaffected as R varies. Also, the Condon appproximation holds well here: $A_H/A_D = 2$; see Section 2. For H-bonds with moderate strength, the ratio increases reaching a maximum at $R \simeq 2.53$ Å. The position of this maximum roughly matches with the minimum of the frequency ratio in Figure 8 of Ref. [20]. For still stronger H-bonds, the intensity ratio declines and becomes ~ 1.7 at very short R. This is attributed to the square-well-like behaviour of the potential for this range of R. [20] (For a square-well potential, the vibrational wavefunctions are independent of mass while the transition frequencies are mass dependent. Thus the ratio of intensities will mainly be due to the frequency ratio, which is approximately 2.)

Another important aspect of the isotope effect is the secondary geometric isotope effect (SGIE) where the O-O equilibrium distance is changed upon substituting H by D (Section 2.2). This modifies the adiabatic potential, which, in turn, also affects the intensity. Therefore, the experimental quantity that we need to calculate is $A_H(R_H)/A_D(R_D)$, where R_D is different from R_H due to SGIE. The red curve of Figure 4 shows this ratio. Evidently, this ratio is overall larger compared to the one without SGIE. The maximum is shifted to slightly lower R, and interestingly also roughly corresponds to the H/D frequency ratio minimum calculated with SGIE in Figure 8 of Ref. [21]. Bratos et al. [5] quotes the A_H/A_D ratio to be about 2, 2.6, and 3-5 for weak, moderate, and strong bonds, respectively. These are in agreement with our results that include the SGIE.

Insight into the observed trend of the A_H/A_D ratio with R can be given by analysing how the integrand of the transition dipole moment, $\phi_{1^+}\mu_g(r)\phi_{0^-}$, varies with r for each isotope at different R values. This product function is plotted in Figure 5 for O-O distances in the weak ($R = 2.8$ Å) and fairly strong ($R = 2.5$ Å) H-bond regions. The H (black) and D (blue) curves are without the inclusion of the SGIE. They are different essentially because H experiences larger anharmonicity effects than D. The wavefunctions for H have a greater spread than those for D. With $\mu_g(r)$ being the same for both, the product function plotted for H in both panels of Figure 5 have larger positive than negative areas compared to those for D. Therefore, the transition dipole integral is higher for H than D. On including the SGIE $\mu_{1^+0^-}$ (red curves), one sees very little change for weak bonding; the integrands with and without this effect are rather similar.

13

For strong H-bonds, there is a clear difference. The resulting integrals for D are smaller and so A_H/A_D is higher.

3.6. Overtone intensity

Figure 6 shows the intensity of the $2^+ \leftarrow 0^-$ transition as a function of R for a symmetric H-bond. Its intensity for a monomeric OH (at $R = 6.0$ Å for our model) is about 0.32 km/mol. It has a complicated non-monotonic dependence on R. The inset shows that with decreasing R the intensity initially drops to zero at about 2.96 Å, and thereafter rises rapidly. This initial overtone suppression occurs at a distance somewhat larger than anticipated based on prior works, which indicate suppression up to at least 2.8 Å. We shall see further below that this might be a consequence of asymmetric H-bonds studied in those works. Continuing to smaller R or stronger H-bonds, we find the transition intensity going up to ~ 17 km/mol, which is about a 50-fold enhancement. That the overtone is not suppressed at all distances, but instead increases to significant values compared to that for a free OH oscillator, is a new finding in this work.

As argued in Section 3.1, the $1^- \leftarrow 0^+$ transition may also be labelled as the overtone for strong H-bonds. For example, at 2.45 Å, it is this transition that is about twice the fundamental, while the $2^+ \leftarrow 0^-$ transitions has thrice the frequency. Figure 7 gives the variation for the intensity of this transition with R. It is of significance only when $R \lesssim 2.6$ Å, when it becomes distinct from the fundamental, due to observable tunnel splitting. When this happens the intensity has a highly non-monotonic variation with R, quite distinct from the monotonic increase with bond strength of the $2^+ \leftarrow 0^-$ transition. In this region ($R \leq 2.6$ Å), the $1^- \leftarrow 0^+$ transition has a generally larger, but rapidly dropping, intensity compared to the $2^+ \leftarrow 0^-$ transition; note the ordinate scale of the two plots. Thus observing both frequency range (Figure 1) and intensity variation (Figures 6 and 7) will help distinguish the two overtones.

We now return to the weak H-bonding region, and discuss the effect of asymmetry on the double well potential. Plots of the $2 \leftarrow 0$ transition using $V_o = 40$, 50, and 75 kcal/mol are shown in Figure 8. Note that the applied V_o are all sizeable compared to the OH dissociation energy (Morse parameter D here is 120 kcal/mol). Although the shifted right diabat lies higher than the Morse overtone level (about 25 kcal/mol above the potential minimum) for all cases, the overtone intensity trends are different for each V_o. Importantly, though, all of them lower the O-O distance range for overtone suppression to at least 2.8 Å. It is difficult to ascertain the precise cause of this change, but our calculations show that overtone properties are rather sensitive to the shape of the anharmonic potential and the resulting $\mu_g(r)$ as well. Indeed, it is this sensitivity that leads to the curious trend in Figure 6.

However, a qualitative understanding of the trends between the three V_o values of Figure 8 may be obtained through the work of di Paolo et al.[14]. They give the overtone intensity to be proportional to $(\mu_g' b + \mu_g'')^2$. (See the end of Section 3.2 for the notation.) As such, with $b < 0$ and the derivatives having the same sign, the two parts of the sum compete with each other. (This leads to a qualitative explanation for overtone suppression.) As V_o increases,

14

we may expect the anharmonicity parameter b to decrease (towards its Morse value). Assuming that the dipole derivatives are approximately constant over the chosen V_o range, the overtone intensity would increase with V_o at a given R. The plots also show the overtone is less suppressed at higher V_o.

3.7. Senstivity to the dipole function for the diabatic states

The shape of the ground state dipole function $\mu_g(r)$ [Eq. (12)] is dependent on that of the diabatic dipole function, $\mu_0(r)$. In Sec. 2.4, we have discussed the reasons for our choice of the Mecke form, Eq. (14), for $\mu_0(r)$. We presently analyse the result of varying the parameter r^* in the Mecke function on the fundamental and overtone intensities of the H-bonded complex. We first discuss small variations around the Lawton-Child value of $r^* = 0.6$ Å, followed by larger variations where $r^* > r_0$, $r_0 = 0.96$ Å being the equilibrium OH distance.

The value of r^* marks the position of the Mecke function maximum. When varied, it is useful to know how the first and second derivatives of μ_0 change at $r = r_0 = 0.96$ Å. Figure 9 shows that the first derivative $\mu_0'(r_0)$ changes within about 20% as r^* is varied from 0.5 to 0.7 Å. However, the second derivative $\mu_0''(r_0)$ changes more substantially, doubling at 0.7 Å and reducing at 0.5 Å to 20% of the original value (at $r^* = 0.6$ Å). This suggests that changing r^*, and hence $\mu_g(r)$, might result in a noticeable but fractional change on the fundamental intensity, but substantially alter the intensity of the overtone, and thereby their ratio as well.

Figure 10 shows the $1^+ \leftarrow 0^-$ fundamental (left panel) and $2^+ \leftarrow 0^-$ overtone (right panel) intensities as a function of R for different r^* values. For the fundamental, the overall intensity pattern is similar at different r^* in the 0.5-0.7 range. The extent of amplification increases at short R (strong bonds) for larger r^*. However, we find that the intensities for successive r^* values differ by about 10-20% at both large and small R. In effect, variation in the fundamental intensities with the shape parameter of the diabatic dipole function is modest. Note also a trend reversal at $R \sim 2.75$ Å, better seen in the inset. At $R \simeq 3.0$ Å, the fundamental intensity is lower for larger r^*, consistent with the Mecke function derivatives discussed above. However, the opposite trend is seen for lower R. A brief analysis of this observation is presented in the Appendix.

For the overtone, the right panel of Figure 10 shows that the overall shape remains about the same. But the intensity drops strongly as r^* decreases between 0.7 and 0.52 Å. This trend appears in agreement with the variation in $\mu_0''(r_0)$ discussed at the start of this Section (see Figure 9). However, the inset shows a trend reversal for weak H-bonds, although the $\mu_0''(r_0)$-based trends is expected to be valid here. We do not analyse this further, save to note that overtone trends are sensitive to the details of $\mu_g(r)$. Another aspect that the inset points to is that the extent and range of overtone suppression in the weak H-bonding range is a sensitive function of r^*.

We now turn to larger changes in r^*, from 0.6 until 1.3 Å. In order to compare the results on an even footing, we impose the constraint that $\mu_0(r_0)$ remains the same at all r^*. This implies that the prefactor μ^* of the Mecke form must change between two r^* values according to the relation $\mu_b^* = \mu_a^* \exp\left[r_0(1/r_b^* - 1/r_a^*)\right]$.

15

This constraint was not applied in the analyses presented earlier in this section for simplicity. However, the general trends discussed still remain the same: The plots for $r^* = 0.52$ (0.7) would be scaled up (down) by 28% (20%), whereby all curves in Figure 10 would look closer together at small R.

Figure 11 show the trends in the fundamental (left panel) and overtone (right panel) intensity. The fundamental is still enhanced for strong H-bonds. However, there is a distinct change on either side of $r^* = r_0$ for weak H-bonds (large R). The fundamental is expected to have almost no intensity for $r^* = 1\text{Å} \simeq r_0$ since this is the maximum of the Mecke form. For larger r^*, the intensities are clearly much weaker than those for $r^* < r_0$. Furthermore, the fundamental intensity gets suppressed in the weak H-bond region (inset of left panel), becoming almost zero at some value of R.

The overtone (right panel) also shows a different trend. For $r^* > r_0$, it appears to monotonically increase, even in the weak H-bonding region. This is to be contrasted with the inset in Fig. 6 which indicates a suppression of intensity. Also, the overtone limiting values at large R are rather large and of comparable magnitude to the fundamentals. The present findings suggest that, at least within the limits of the Mecke dipole form, results obtained with $r^* > r_0$ are not in line with literature results on H-bond trends, while those with $r^* < r_0$ are. It should be stressed that one of our main results is independent of the relative size of r^* and r_0: the overtone intensity is enhanced for medium and strong bonds.

We have also analysed the isotope intensity ratio, A_H/A_D, at different r^* values without SGIE. For strong and medium-strong H-bonds, this ratio is akin to the black curve in Figure 4 but with a larger peak value (~ 3 at $r^* = 0.6$ and ~ 4.5 at $r^* = 1.2$) that rises roughly linearly with r^*. The peak position also shifts to $R \sim 2.6$ Å over the r^* range. These variations, though notable, are only gradual. Furthermore, our main point still stands: the isotope ratio is a non-monotonic function of R and can have values significantly different from the harmonic value of 2.

4. Comparison with previous work

We have already noted in earlier sections that that our results for the fundamental enhancement in Figure 2 (solid line) and the corresponding A_H/A_D ratio in Figure 4 with SGIE are in overall agreement with experimental ranges summarised by Bratos et al. [5] (see Sections 3.2 and 3.5). We now consider some specific molecular systems. All comparisons made below are using the Lawton-Child parameters in the Mecke function.

4.1. Symmetric H-bonds

Bournay and Marechal [65] measured the isotope intensity ratio for acetic acid dimers in the gas phase (which have $R \simeq 2.68$ Å[66]), finding a ratio of 2 ± 0.2 for the transition probabilities (i.e., $|\mu_{fi}|^2$). Owing to a marked departure from the harmonic value $\sqrt{2}$, they suggested the value to be anomalous, and

16

attributed it to a breakdown of the Born-Oppenheimer approximation. However, our model is within this approximation. At that O-O distance, Fig. 4 gives $A_H/A_D \approx 2.6$, while the frequency ratio $\nu_H/\nu_D \approx 1.3$ from Figure 8 of Ref. [20]. This yields a transition probability of about 2.0, which agrees with their measurements. In contrast, our estimate of about 5 for the H isotope's $|\mu_{fi}|^2$ enhancement compared to the monomer is much lower than their experimental estimate of about 32.

A number of theoretical and experimental studies have been performed on the Zundel cation, $H_5O_2^+$, which has $R \simeq 2.5$ Å. More recently, Tan and Kuo [67] studied $(CH_3OH)_2H^+$, which has $R \simeq 2.4$ Å. For the Zundel cation, one of the peaks around 1000 cm^{-1} is identified with the proton transfer motion, which would correspond to the $0^- \leftarrow 0^+$ transition in the notation of present work; see our footnote in Ref. [68]. Unfortunately, an experimental measurement of the absolute intensity seems unavailable. Theoretical studies also give the relative intensities of this mode to be 3-10,[69] 8, [70] and 20-40 [71] times the intensity of the OH stretches of the end groups. For $(CH_3OH)_2H^+$, the OH stretch at 1010 cm^{-1} (also $0^- \leftarrow 0^+$ in our notation) was computed to have an intensity of 2567 km/mol [67].

In the present work for $R = 2.5$ Å and 2.4 Å, the $0^- \leftarrow 0^+$ transition has frequencies of about 164 and 750 cm^{-1}, respectively. Clearly, these are lower than those of the aforementioned works. The corresponding intensities are about 335 and 600 km/mol, or enhancements of about 9 and 15. (Note that these are relative to $1^+ \leftarrow 0^-$ at $R = 6.0$ Å.) At the same R values, $1^+ \leftarrow 0^-$ frequencies are 1620 and 1780 cm^{-1}, which err on the higher side compared to the Zundel and $(CH_3OH)_2H^+$ cations. The corresponding intensities are about 625 and 950 km/mol, i.e. 16 and 24-fold enhancement.

We end this section with a brief comparison with a particle in a box (PIB) model. For short, strong H-bonds the potential appears similar to that for a PIB of width $L = R - 2r_0$ with quantum numbers $n = 1, 2, 3, \ldots$ [20]. The corresponding transition dipole moment for a transition $n_f \leftarrow n_i$, is only non-zero when $n_f - n_i$ is odd, for which $A_{if} \propto (n_f^2 n_i^2)/(n_f^2 - n_i^2)^3$ is box-length independent. Here, the three transitions $3 \leftarrow 2$, $4 \leftarrow 1$, and $5 \leftarrow 2$, in the PIB. correspond to $1^+ \leftarrow 0^-$, $1^- \leftarrow 0^+$, and $2^+ \leftarrow 0^-$, respectively, in the strong H-bond case. In the PIB, the three transitions have the intensity ratios about 60:1:2. Figures 2, 6 and 7 suggest that the the ratios are roughly comparable, but are still clearly R-dependent unlike the PIB case.

4.2. Asymmetric H-bonds

The molecular system discussed below are weak H-bonds. For numerical comparisons, we will use our asymmetric model with $V_o = 50$ kcal/mol. Note, however, that this choice of V_o is not special. Our results do vary somewhat with V_o, as Figure 8 demonstrates. For the fundamentals alone, we additionally quote our symmetric model results for contrast. Also, if the H-bonded O-O distance was not directly available from the cited work, it was estimated using the given OH fundamental red-shift and Figure 1 .

17

For the fundamental of ethanol dimers, Provencal et al. [26] calculated an enhancement of 10-20 relative to the monomer in the double harmonic approximation. For intramolecularly H-bonded propane- and butanediol, Howard and Kjaergaard [9] report the OH stretch intensity to be enhanced 4-11 times for different conformers. These H-bonds have $R \simeq 2.8 - 2.9$ Å, for which our enhancement factors are 1.3-1.5 for the symmetric model and 1.07-1.12 for the asymmetric model. Suhm and co-workers' [10] experiments on 2,2,2-trifluoroethanol dimers show an intensity enhancement of 4.0 ± 0.8 for the fundamental of the donor O-H compared to the acceptor O-H. Our values are about 1.26 and 1.04 for the symmetric and asymmetric cases. For the water dimer, the O-O distance is close to 3.0 Å[72]. The asymmetric stretch fundamental enhancement is 2-3 times that of the monomer [29, 34, 35]. Our values are 1.1 and 1.03 from the symmetric and asymmetric models. We parenthetically note that recent studies have noted a strong experimental (theoretical) enhancement of the symmetric stretch, from about 3 (4) km/mol to about 140 (160) km/mol, upon dimer formation [35]. In general, the enhancement from our calculation for $R \gtrsim 2.7$ Å is at most ~ 2 with the symmetric model and ~ 1.2 with the asymmetric model (see inset of Figure 2), both of which are smaller than values in the literature.

For the same molecules, however, our overtone suppression estimate compares somewhat more favourably. Suhm and coworkers reported a value of A/A_{free} for 2,2,2-trifluoroethanol dimer to be 0.3 ± 0.1 [10]. Our estimate is 0.63. Calculations by Howard and Kjaergaard [9] for propane- and butanediols indicate a suppression from 0.43 to 0.15, with lower values for butanediols. Our estimates are consistent with this relative ordering of magnitudes and in the range 0.41 to 0.20. In general, literature values of A/A_{free} for the overtone are about 0.5 to 0.1, the smaller values pointing to stonger H-bonds. Figure 8 indicates (for R between 2.8 and 3.0 Å) that our estimates are in about that range, allowing for variation of the asymmetry parameter V_o. For the water dimer ($R \simeq 3$Å), our suppression ratios with the asymmetric and symmetric models are 0.7 and 0.13, respectively. Kjaergaard et al. [28, 29] compute the ratio to be as low as 0.02. They show [28] this to be a consequence of near cancellation of the linear and quadratic parts in the dipole matrix element expansion.

Finally, we discuss another metric, namely the fundamental-to-overtone intensity ratio, A_1/A_2. This ratio is typically about 10 for monomers, and is reported to increase by over an order of magnitude with H-bonding [10, 11, 25] in the weak region. For 2,2,2-trifluoroethanol dimer, Scharge et al. [10] report $A_1/A_2 = 400 \pm 100$ and 30 ± 10 for the donor and acceptor O-H bonds, respectively. Our A_1/A_2 ratios are about 366 and 218, respectively. The experimental monomer ratio of 13 ± 2 is smaller than our ($R = 6.0$ Å) estimate of about 122. A more recent work from the Suhm group on the dimers of methanol, ethanol and t-butyl alcohol [11] gives the A_1/A_2 ratio for the donor O-H as 320 ± 90, 400 ± 100 and 1000 ± 400. Using values of R deduced from redshifts, our ratios are ≈ 493, 583, and 711, in reasonable accord with experiment.

We also mention that some O-H$\cdots$Y-type asymmetric complexes have been analysed, e.g. $F^- \cdot H_2O$ [73] and $Cl^- \cdot H_2O$ [74] in theoretical studies. The former has a strong H-bond, for which an OH fundamental intensity enhancement

18

of about 35 was computed (in the double harmonic approximation). For the chloride complex, it was found to be 50 using an anharmonic treatment. It also showed overtone suppression of 0.35. Recent studies on alcohol-amine complexes with OH$\cdots$N H-bonds have reported fundamental enhancements over a factor of 50 [75]. We have not attempted any numerical comparisons for these cases, since our model is parametrized for O-H$\cdots$O systems.

5. Summary and Concluding Remarks

We have discussed the intensity variation of the fundamental and overtone transitions in O-H$\cdots$O type H-bonds. The results are based on a diabatic two-state potential model and a Mecke form for the diabatic dipole moment. These yield a ground adiabat and associated adiabatic dipole moment along the H-atom transfer coordinate. The latter along with one-dimensional vibrational wavefunctions were used to compute the intensities for a range of O-O distances. Over this range, the H-bond varies from weak to strong. Also analysed are the role of donor-acceptor asymmetry (i.e. difference in their pK_a's) as well as the effect of the shape of the Mecke function for the dipole moment.

For the OH fundamental, we find that the intensity is enhanced compared to the free OH over all relevant O-O distances, ranging from a factor of under 2 for weak H-bonds to about 20 for strong bonds. We show that the non-linearity of the dipole moment is important, especially for medium and strong H-bonds, and therefore the Condon approximation is not suitable. The H/D isotope effect was analysed in terms of the fundamental intensity ratio, which is found to be non-monotonic with H-bond strength. A maximum occurs for this ratio at the donor-acceptor distance R of about 2.5 Å, and the secondary geometric isotope effect plays an important role in the height and position of this maximum. For the OH overtone, our model finds intensity suppression for weak H-bonds, and shows variability in magnitude and R_{OO} range depending on whether we consider symmetric or asymmetric bonds. For medium and strong H-bonds, enhancements in the intensity are seen with the symmetric model, going up to 50 times the free OH value. This new finding suggests that overtones should be experimentally visible for such H-bonds compared to those in the weak H-bonded region.

Our results are generally consistent in trends but differ in numbers with previous work, including both experimental and theoretical studies. In particular, our enhancements in fundamental intensities for weak H-bonds are clearly lower. Comparisons of overtone suppression in the same region with the asymmetric model fare somewhat better. We have also analysed how our results vary with the shape of the dipole moment. Small parameter variations lead to modest fractional change in the intensity of the fundamental, but to larger changes for the overtone. Larger variations give similar results for strong H-bonds, but qualitatively different results for weak bonds.

Studies of H-bond intensities offer an excellent point of comparison for experiment and theory, owing to the large spread of bonding strengths and topologies. In the present context of O-H$\cdots$O H-bonds, with a few exceptions such as $H_5O_2^+$

and $(CH_3OH)_2H^+$, most detailed studies have mainly focussed on specific systems in the weak H-bonding regime. Experiments on symmetric medium and strong H-bonded systems are desirable to test our main results. Some possible candidates are carboxylic acid dimers ($R \simeq 2.45$ Å), $HCrO_2$ ($R \simeq 2.49$ Å), porphycenes[76], and proton sponges[77], for which the fundamental, first overtone, and isotope effect could be measured and analysed. It must also be noted that measurement of absolute intensities for comparison with theory are difficult, owing to wide spectra sometimes spanning several hundred wavenumbers. Another attendant difficulty is knowing the proportion of dimers in a sample. Slightly asymmetric biomolecular systems with strong H-bonds that could be investigated include mutated GFP[78], photoactive yellow protein[79] and the enzyme KSI[80].

Acknowledgments

Appendix A. Dipole shape and scale contributions to infrared absorption intensity

Figure 10 shows the fundamental intensity variation when the Mecke parameter r^* is changed to a small extent. The traces at the bottom right of the plot (expanded in the inset) show that there is point of crossover. At $R = 3.0$ Å, large r^* values are associated with lower intensity. But at $R \lesssim 2.7$ Å, the opposite trend is seen. We briefly analyse this feature here.

All components of the transition moment integral $\langle \phi_{1+} \mid \mu_g(r) \mid \phi_{0-} \rangle$ vary with R, but only $\mu_g(r)$ changes with r^*. We rewrite the integral as $\mu_{g,n} \langle \phi_{1+} \mid \mu_g(r)/\mu_{g,n} \mid \phi_{0-} \rangle = \mu_{g,n}\langle S \rangle$. We take $\mu_{g,n} \equiv \mu_g(r = r_{node})$, where r_{node} is the (non-central) node of the wavefunction product (shown in Figure 3) for that R. Note that r_{node} does not shift with r^* at a given R, and therefore provides a common reference point at that R. In this manner, the transition moment is separated into a shape part, $\langle S \rangle$ and an overall magnitude, $\mu_{g,n}$. Though not shown, we found that plots of $\mu_g(r)/\mu_{g,n}$ for various R and r^* look nearly the same. Table A.1 shows the intensity contributions of these pieces for $r^* = 0.56$ and 0.64 Å, relative to those at $r^* = 0.6$ Å. For the shorter distances ($R = 2.6$ and 2.4 Å), the relative intensities (A ratios) are about the same as the relative $\mu_{g,n}^2$. The ratio of $|\langle S \rangle|^2$ is nearly unity, so the shape of the dipole function plays a minor role. However, for weak H-bonds, the shape appears to play a role. At $R = 2.8$ Å, it overrides the effect of $\mu_{g,n}$. The above suggests that the interplay of shape and scale contributions results in the crossover.

We note that all the traces in Figure 10 are a result of changing only r^* in the Mecke function. In the latter half of Section 3.7 and in Figure 11, the effect of changing μ^* as well using a constraint relation (which ensures that $\mu_0(r_0)$ does not change) is discussed. In the present context, the numerical results are affected only to the extent that both the A ratios and $\mu_{g,n}$ ratios are scaled by a single number for a given r^*. This number is the ratio of the μ^*s, which is about

Table A.1: Contribution to the fundamental intensity at different value of Mecke parameter r^*. Compared are the total intensity (A), the scale factor ($\mu_{g,n}$) and the matrix element of $\mu_g(r)/\mu_{g,n}$, denoted $\langle S \rangle$. All results are reported as ratios relative to the results for $r^* = 0.6$; the ^{o} superscript in the table header indicates the value of the quantity for $r^* = 0.6$. The final column is obtained as a ratio of the middle two.

R (Å)	A/A^o	$|\mu_{g,n}/\mu_{g,n}^o|^2$	$|\langle S \rangle/\langle S \rangle^o|^2$
		$r^* = 0.56$	
2.8	1.02	0.89	1.15
2.6	0.87	0.89	0.97
2.4	0.83	0.80	1.03
		$r^* = 0.64$	
2.8	0.95	1.11	0.86
2.6	1.13	1.10	1.02
2.4	1.12	1.18	0.94

1.2 (0.9) for $r^* = 0.56$ (0.64) Å. Although the location of the crossover would shift a little (outward), the qualitative aspects of the above analysis remain unchanged.

[1] E. Arunan, G. R. Desiraju, R. A. Klein, J. Sadlej, S. Scheiner, I. Alkorta, D. C. Clary, R. H. Crabtree, J. J. Dannenberg, P. Hobza, et al., Defining the hydrogen bond: An account (iupac technical report), Pure Appl. Chem. 83 (8) (2011) 1619–1636.

[2] C. Pimentel, George, L. McClellan, Aubrey, The Hydrogen Bond, W. H. Freeman And Company, 1960.

[3] Y. Marechal, A. Witkowski, Infrared spectra of h-bonded systems, J. Chem. Phys. 48 (1968) 3697–3705.

[4] S. Bratos, Profiles of hydrogen stretching ir bands of molecules with hydrogen bonds: A stochastic theory. I. Weak and medium strength hydrogen bonds, J. Chem. Phys. 63 (1975) 3499–3509.

[5] S. Bratos, H. Ratajczak, P. Viot, Properties of h-bonding in the infrared spectral range, in: Hydrogen-Bonded Liquids, Springer, 1991, pp. 221–235, [Note: The intensity ratio for isotopes in this reference appears to be the square of the dipole matrix element ratio alone. We use their values after multiplication with the frequency ratio they have given].

[6] F. Fillaux, Theoretical model for calculations of infrared and raman band profiles of strong hydrogen bonds in ordered media, Chem. Phys. 74 (3) (1983) 395–404.

[7] A. Iogansen, Direct proportionality of the hydrogen bonding energy and the intensification of the stretching [nu](XH) vibration in infrared spectra,

Spectrochim. Acta A 55 (7-8) (1999) 1585–1612, [Note: This review was apparently the first one on the topic by the author in an English language journal. The original works in Russian, Refs. 4 and 5 of the current reference, were published in the 1960s.].

[8] C. Burnham, G. Reiter, J. Mayers, T. Abdul-Redah, H. Reichert, H. Dosch, On the origin of the redshift of the OH stretch in Ice Ih: evidence from the momentum distribution of the protons and the infrared spectral density, Phys. Chem. Chem. Phys. 8 (34) (2006) 3966–3977.

[9] D. L. Howard, H. G. Kjaergaard, Influence of intramolecular hydrogen bond strength on oh-stretching overtones, J. Phys. Chem. A 110 (2006) 10245–10250.

[10] T. Scharge, D. Luckhaus, M. A. Suhm, Observation and quantification of the hydrogen bond effect on o-h overtone intensities in an alcohol dimer, Chem. Phys. 346 (13) (2008) 167 – 175.

[11] F. Kollipost, K. Papendorf, Y.-F. Lee, Y.-P. Lee, M. A. Suhm, Alcohol dimers – how much diagonal OH anharmonicity?, Phys. Chem. Chem. Phys. 16 (30) (2014) 15948.

[12] H. Ratajczak, W. Orville-Thomas, C. Rao, Charge transfer theory of hydrogen bonds: relations between vibrational spectra and energy of hydrogen bonds, Chem. Phys. 17 (2) (1976) 197–216.

[13] M. Rozenberg, The hydrogen bond – practice and QTAIM theory, RSC Adv. 4 (2014) 26928.

[14] T. D. Paolo, C. Bourdéron, C. Sandorfy, Model Calculations on the Influence of Mechanical and Electrical Anharmonicity on Infrared Intensities: Relation to Hydrogen Bonding, Can. J. Chem. 50 (19) (1972) 3161–3166.

[15] G. E. Hilbert, O. R. Wulf, S. B. Hendricks, U. Liddel, The hydrogen bond between oxygen atoms in some organic compounds, J. Am. Chem. Soc. 58 (4) (1936) 548–555.

[16] E. Heller, The many faces of tunneling, J. Phys. Chem. A 103 (49) (1999) 10433–10444.

[17] K. K. Lehmann, A. M. Smith, Where does overtone intensity come from?, J. Chem. Phys. 93 (9) (1990) 6140–6147.

[18] E. S. Medvedev, Towards understanding the nature of the intensities of overtone vibrational transitions, J. Chem. Phys. 137 (17) (2012) 174307.

[19] R. H. McKenzie, A diabatic state model for donor-hydrogen vibrational frequency shifts in hydrogen bonded complexes, Chem. Phys. Lett. 535 (2012) 196–200.

[20] R. H. McKenzie, C. Bekker, B. Athokpam, S. G. Ramesh, Effect of quantum nuclear motion on hydrogen bonding, J. Chem. Phys. 140 (17) (2014) 174508.

[21] R. H. McKenzie, B. Athokpam, S. G. Ramesh, Isotopic fractionation in proteins as a measure of hydrogen bond length, J. Chem. Phys. 143 (4) (2015) 044309.

[22] R. Mecke, Dipolmoment und chemische Bindung, Z. Electrochem. 54 (1) (1950) 38–42.

[23] P. F. Bernath, Spectra of Atoms and Molecules, 2nd Edition, Oxford University Press, 2005.

[24] W. Zou, D. Cremer, Properties of local vibrational modes: the infrared intensity, Theor. Chem. Acc. 133 (3) (2014) 1451.

[25] J. Phillips, J. Orlando, G. Tyndall, V. Vaida, Integrated intensities of OH vibrational overtones in alcohols, Chem. Phys. Lett. 296 (3-4) (1998) 377–383.

[26] R. A. Provencal, R. N. Casaes, K. Roth, J. B. Paul, C. N. Chapo, R. J. Saykally, G. S. Tschumper, H. F. Schaefer, Hydrogen bonding in alcohol clusters: a comparative study by infrared cavity ringdown laser absorption spectroscopy, J. Phys. Chem. A 104 (7) (2000) 1423–1429.

[27] G. R. Low, H. G. Kjaergaard, Calculation of oh-stretching band intensities of the water dimer and trimer, J. Chem. Phys. 110 (18) (1999) 9104–9115. doi:10.1063/1.478832.

[28] H. G. Kjaergaard, G. R. Low, T. W. Robinson, D. L. Howard, Calculated oh-stretching vibrational transitions in the waternitrogen and wateroxygen complexes, J. Phys. Chem. A 106 (38) (2002) 8955–8962. doi:10.1021/jp020542y.

[29] H. G. Kjaergaard, A. L. Garden, G. M. Chaban, R. B. Gerber, D. A. Matthews, J. F. Stanton, Calculation of vibrational transition frequencies and intensities in water dimer: Comparison of different vibrational approaches, J. Phys. Chem. A 112 (18) (2008) 4324–4335. doi:10.1021/jp710066f.

[30] D. P. Schofield, J. R. Lane, H. G. Kjaergaard, Hydrogen bonded oh-stretching vibration in the water dimer, J. Phys. Chem. A 111 (4) (2007) 567–572. doi:10.1021/jp063512u.

[31] Y. Bouteiller, J. Perchard, The vibrational spectrum of (h2o)2: comparison between anharmonic ab initio calculations and neon matrix infrared data between 9000 and 90 cm1, Chem. Phys. 305 (13) (2004) 1 – 12. doi:10.1016/j.chemphys.2004.06.028.

[32] Y. Bouteiller, B. Tremblay, J. Perchard, The vibrational spectrum of the water dimer: Comparison between anharmonic ab initio calculations and neon matrix infrared data between 14,000 and 90 cm1, Chem. Phys. 386 (13) (2011) 29 – 40. doi:10.1016/j.chemphys.2011.05.014.

[33] M. N. Slipchenko, K. E. Kuyanov, B. G. Sartakov, A. F. Vilesov, Infrared intensity in small ammonia and water clusters, J. Chem. Phys. 124 (24) (2006) 241101. doi:10.1063/1.2216712.

[34] K. Kuyanov-Prozument, M. Y. Choi, A. F. Vilesov, Spectrum and infrared intensities of OH-stretching bands of water dimers, J. Chem. Phys. 132 (2010) 014304.

[35] A. F. Silva, W. E. Richter, R. E. Bruns, Quantum theory of atoms in molecules/chargecharge fluxdipole flux interpretation of fundamental vibrational intensity enhancements on h-bond formation of water trimer, Chem. Phys. Lett. 610-611 (2014) 14 – 18. doi:10.1016/j.cplett.2014.07.002.

[36] E. U. Condon, Nuclear motions associated with electron transitions in diatomic molecules, Phys. Rev. 32 (6) (1928) 858.

[37] S. Wang, Generalization of the thomas-reiche-kuhn and the bethe sum rules, Phys. Rev. A 60 (1) (1999) 262–266.

[38] J. Vazquez, J. F. Stanton, Simple(r) algebraic equation for transition moments of fundamental transitions in vibrational second-order perturbation theory, Mol. Phys. 104 (3) (2006) 377–388.

[39] S. Banik, M. Durga Prasad, On the spectral intensities of vibrational transitions in polyatomic molecules: role of electrical and mechanical anharmonicities, Theor. Chem. Acc. 131 (11) (2012) 1282.

[40] J. Schmidt, S. Corcelli, J. Skinner, Pronounced non-condon effects in the ultrafast infrared spectroscopy of water, J. Chem. Phys. 123 (4) (2005) 044513.

[41] A. B. McCoy, T. L. Guasco, C. M. Leavitt, S. G. Olesen, M. A. Johnson, Vibrational manifestations of strong non-condon effects in the $H_3O^+ \cdot X_3$ (x= ar, N_2, CH_4,H_2O) complexes: A possible explanation for the intensity in the "association band" in the vibrational spectrum of water, Phys. Chem. Chem. Phys. 14 (20) (2012) 7205.

[42] G. Gilli, P. Gilli, The Nature of the Hydrogen Bond, Oxford U.P., Oxford, 2009.

[43] W. H. Thompson, J. T. Hynes, Frequency shifts in the hydrogen-bonded oh stretch in halide-water clusters. the importance of charge transfer, J. Am. Chem. Soc. 122 (26) (2000) 6278–6286.

[44] D. T. Colbert, W. H. Miller, J. Chem. Phys. 96 (1992) 1982.

24

[45] J. M. Robertson, A. R. Ubbelohde, Structure and thermal properties associated with some hydrogen bonds in crystals. i. the isotope effect, Proc. Roy. Soc. A 170 (941) (1939) 222–240.

[46] M. Ichikawa, Hydrogen-bond geometry and its isotope effect in crystals with OHO bonds—revisited, J. Mol. Struct. 552 (1-3) (2000) 63–70.

[47] N. Sokolov, M. Vener, V. Savel'ev, Tentative study of the strong hydrogen bond dynamics, J. Mol. Struct. 177 (1988) 93–110.

[48] A. Nitzan, Chemical Dynamics in Condensed Phases: Relaxation, Transfer and Reactions in Condensed Molecular Systems, Oxford University Press, 2006.

[49] I. Schek, J. Jortner, M. L. Sage, Intensities of high-energy molecular C-H vibrational overtones, Chem. Phys. Lett. 64 (1979) 209–212.

[50] R. T. Lawton, M. S. Child, Excited stretching vibrations of water: the quantum mechanical picture, Mol. Phys. 40 (1980) 773–792.

[51] M. Lewerenz, M. Quack, Vibrational overtone intensities of the isolated CH and CD chromophores in fluoroform and chloroform, Chem. Phys. Lett. 123 (3) (1986) 197–202. doi:10.1016/0009-2614(86)80012-4.

[52] W. Jakubetz, J. Manz, V. Mohan, Model preparation of H_2O hyperspherical modes by visible versus infrared multiphoton excitation, J. Chem. Phys. 90 (7) (1989) 3686–3699.

[53] H. Lin, L.-F. Yuan, Q.-S. Zhu, Local mode overtone intensities of SiH4 and GeH4 from a bond dipole model with an ab initio calculated dipole moment surface, Chem. Phys. Lett. 308 (1-2) (1999) 137–141. doi:10.1016/s0009-2614(99)00567-9.

[54] K. R. Lange, N. P. Wells, K. S. Plegge, J. A. Phillips, Integrated intensities of O-H stretching bands: Fundamentals and overtones in vapor-phase alcohols and acids, J. Phys. Chem. A 105 (2001) 3481–3486. doi:10.1021/jp003277u.

[55] K. Takahashi, M. Sugawara, S. Yabushita, Effective one-dimensional dipole moment function for the OH stretching overtone spectra of simple acids and alcohols, J. Phys. Chem. A 109 (19) (2005) 4242–4251. doi:10.1021/jp045041m.

[56] O. Álvarez-Bajo, J. Arias, J. Gómez-Camacho, R. Lemus, An approach to the study of the continuum effects in systems of interacting morse oscillators, Mol. Phys. 106 (9-10) (2008) 1275–1289. doi:10.1080/00268970802206459.

[57] H. G. Kjaergaard, B. R. Henry, Ab initio calculation of dipole moment functions: application to vibrational band intensities of h 2 o, Mol. Phys. 83 (6) (1994) 1099–1116. doi:10.1080/00268979400101811.

[58] J. F. Harrison, Dipole and quadrupole moment functions of the hydrogen halides hf, hcl, hbr, and hi: A hirshfeld interpretation, J. Chem. Phys. 128 (11) (2008) 114320.

[59] J. R. Lane, H. G. Kjaergaard, Xh-stretching overtone transitions calculated using explicitly correlated coupled cluster methods, J. Chem. Phys. 132 (17) (2010) 174304.

[60] T. Steiner, Angew. Chem. Int. Ed. 41 (2002) 48.

[61] A. Novak, Structure and Bonding 18 (1974) 177.

[62] N. Sokolov, M. Vener, V. Savel'ev, J. Mol. Struct. 222 (1990) 365.

[63] P. Gilli, V. Bertolasi, V. Ferretti, , G. Gilli, J. Am. Chem. Soc. 116 (1994) 909.

[64] Based on the O-O distance as a measure, water dimer and alcohol dimers (e.g., methanol, ethanol, trifluoroethanol) are weak H-bonds. Phenol-water complexes with the former as the donor are likely a little stronger [60]. Based on data from X-ray and neutron Diffraction studies [61, 62], carboxylic acid dimers (e.g., acetic and benzoic acid) and dicarboxylic acids (succinic acid), in crytals and likely in liquid and gas phases as well, would fall into the medium to strong category. Strong and very strong H-bonds would be those in $H_5O_2^+$, $H_3O_2^-$ [63], and $(CH_3OH)_2H^+$ [67], and several inorganic acid salts and organic bicarbonate salts [63, 62] as well.

[65] J. Bournay, Y. Marechal, Anomalous isotope effect in the h bonds of acetic acid dimers, J. Chem. Phys. 59 (9) (1973) 5077–5087.

[66] J. L. Derissen, A reinvestigation of the molecular structure of acetic acid monomer and dimer by gas electron diffraction, J. Mol. Struct. 7 (1) (1971) 67–80.

[67] J. A. Tan, J.-L. Kuo, Strong quantum coupling in the vibrational signatures of a symmetric ionic hydrogen bond: The case of (ch3oh) 2h+, J. Phys. Chem. A 119 (46) (2015) 11320–11328.

[68] There is debate about the correct identification of features in the IR spectra, due to large anharmonic and intermode coupling effects, requiring a high-dimensional potential energy surface.

[69] M. V. Vener, O. Kühn, J. Sauer, The infrared spectrum of the o h o fragment of h5o2+: Ab initio classical molecular dynamics and quantum 4d model calculations, J. Chem. Phys. 114 (1) (2001) 240–249.

[70] O. Vendrell, F. Gatti, H.-D. Meyer, Full dimensional (15-dimensional) quantum-dynamical simulation of the protonated water dimer. ii. infrared spectrum and vibrational dynamics, J. Chem. Phys. 127 (18) (2007) 184303.

[71] T. L. Guasco, M. A. Johnson, A. B. McCoy, Unraveling anharmonic effects in the vibrational predissociation spectra of h5o2+ and its deuterated analogues, J. Phys. Chem. A 115 (23) (2011) 5847–5858.

[72] J. A. Odutola, T. R. Dyke, Partially deuterated water dimers: Microwave spectra and structure, J. Chem. Phys. 72 (9) (1980) 5062–5070. doi:10.1063/1.439795.

[73] B. F. Yates, H. F. Schaefer, T. J. Lee, J. E. Rice, Infrared spectrum of f. hivin.. cntdot. h2o, J. Am. Chem. Soc. 110 (19) (1988) 6327–6332.

[74] A. B. McCoy, The role of electrical anharmonicity in the association band in the water spectrum, J. Phys. Chem. B 118 (28) (2014) 8286–8294.

[75] L. Du, K. Mackeprang, H. G. Kjaergaard, Fundamental and overtone vibrational spectroscopy, enthalpy of hydrogen bond formation and equilibrium constant determination of the methanol-dimethylamine complex, Phys. Chem. Chem. Phys. 15 (2013) 10194–10206. doi:10.1039/C3CP50243K.

[76] P. Cika, P. Fita, A. Listkowski, M. Kijak, S. Nonell, D. Kuzuhara, H. Yamada, C. Radzewicz, J. Waluk, Tautomerism in porphycenes: Analysis of rate-affecting factors, J. Phys. Chem. B 119 (6) (2015) 2292–2301. doi:10.1021/jp506150r.

[77] Y. Horbatenko, S. F. Vyboishchikov, Hydrogen motion in proton sponge cations: A theoretical study, ChemPhysChem 12 (2011) 1118–1129.

[78] L. M. Oltrogge, S. G. Boxer, Short hydrogen bonds and proton delocalization in green fluorescent protein (gfp), ACS Cent. Sci. 1 (3) (2015) 148–156.

[79] M. Nadal-Ferret, R. Gelabert, M. Moreno, J. M. Lluch, Are there really low-barrier hydrogen bonds in proteins? the case of photoactive yellow protein, J. Am. Chem. Soc. 136 (9) (2014) 3542–3552. doi:10.1021/ja4116617.

[80] L. Wang, S. D. Fried, S. G. Boxer, T. E. Markland, Quantum delocalization of protons in the hydrogen-bond network of an enzyme active site, Proc. Nat. Acad. Sci. 111 (52) (2014) 18454–18459.
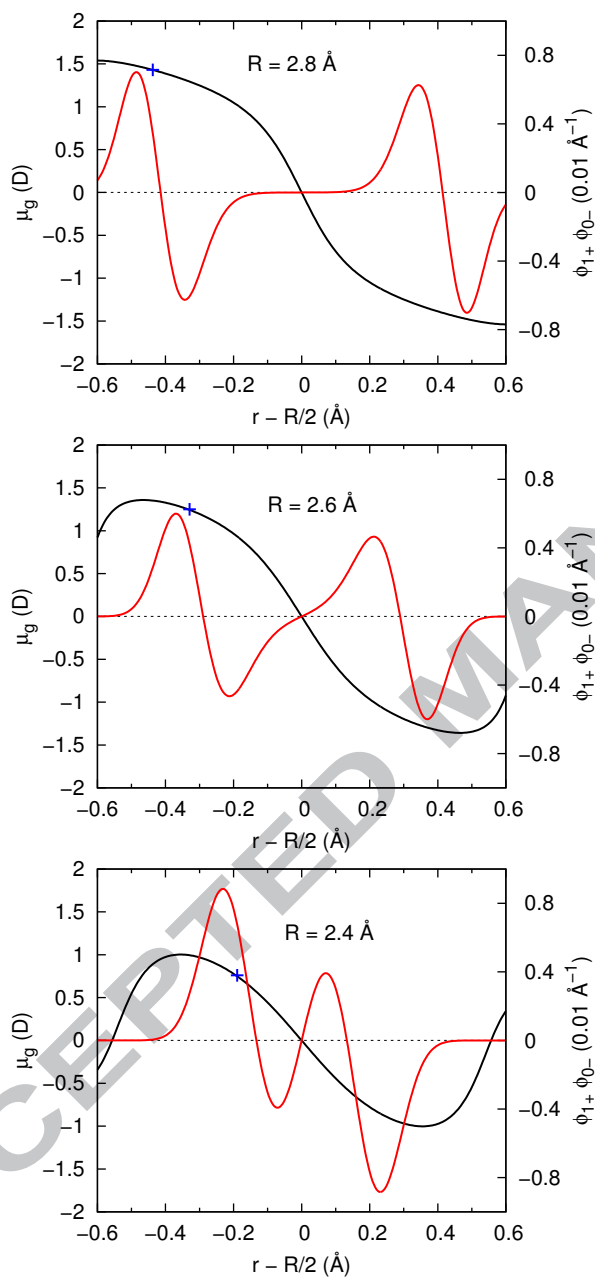
Figure 3: Origin of breakdown of the Condon approximation. Plotted are the dipole moment function $\mu_g(r)$ (black line, left axis) and the wavefunction overlap $\phi_{1+}\phi_{0-}$ (red line, right axis) as a function of $r - R/2$ for $R = 2.8$, 2.6, and 2.4 Å. The product of these two functions is the integrand in the transition dipole matrix element (4). As the H-bond strength increases and R decreases, the wavefunction overlap has significant weight where the dipole function becomes non-linear. That is, as r gets closer to $R/2$, the slope of the dipole function is significantly larger than that at the equilibrium bond length. This non-linearity contributes to the enhanced absorption intensity. The blue plus sign marks the classical minimum of the (left-side of the) double-well for a given R. The dipole derivative in the Condon approximation, Eqn. (5), is evaluated at this point.

28
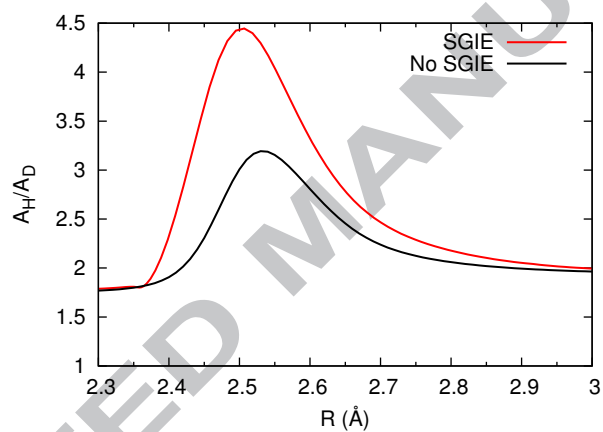
Figure 4: Isotope intensity ratio, A_H/A_D, for the $1^+ \leftarrow 0^-$ transition as a function of the donor-acceptor distance R. For the red (black) curve the secondary geometric isotopic effect (SGIE), i.e, change in the donor-acceptor distance R, is (is not) taken into account. The SGIE enhances the isotope intensity ratio for low-barrier H-bonds.
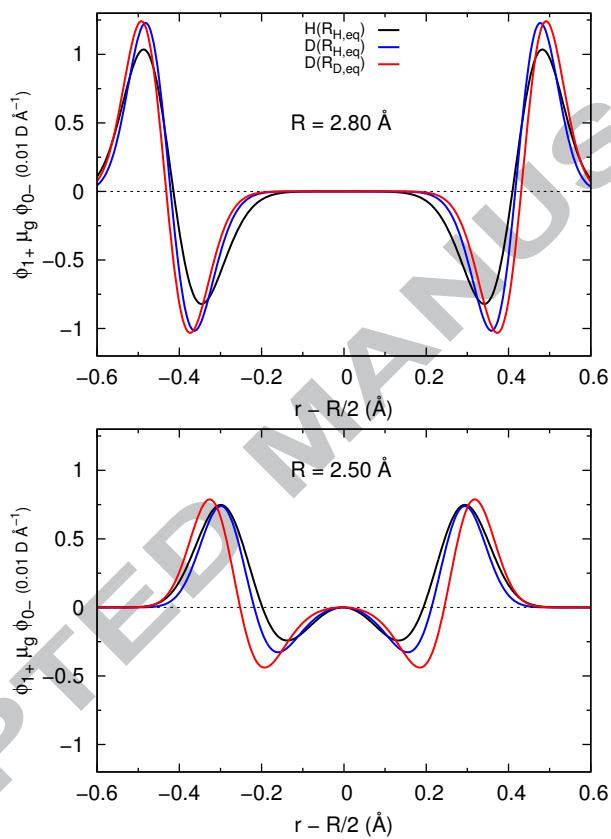
29

Figure 5: Integrand for the transition matrix element $\phi_{1+}\mu_g(r)\phi_{0-}$ for the H and D isotopes for different R. The black curve is for H isotope while red and blue curves are for D isotope with and without the secondary geometric isotope effect (SGIE), respectively. The H-bond is stronger at lower R.
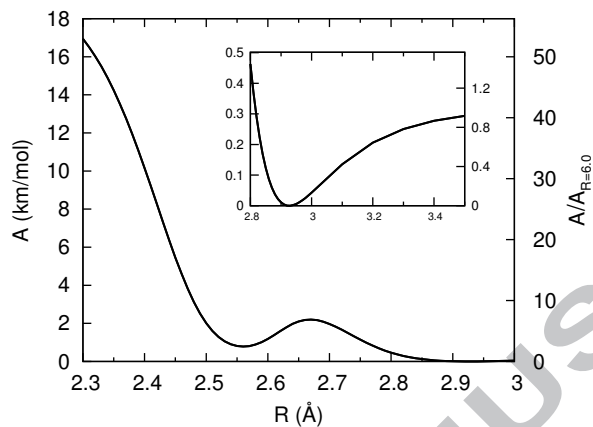
Figure 6: Dependence of the intensity of the $2^+ \leftarrow 0^-$ transition on R. The left axis is the intensity in units of km/mol and the right axis is the intensity scaled by its value for $R = 6.0$ Å (absence of H-bond). This clearly shows the non-monotonic dependence of the overtone intensity on the strength of the H-bond. Furthermore, for medium to strong bonds, significant enhancement of the overtone intensity is possible. The inset shows the trend in the weak H-bonding region. Note that there is some intensity suppression near and above 3.0 Å.
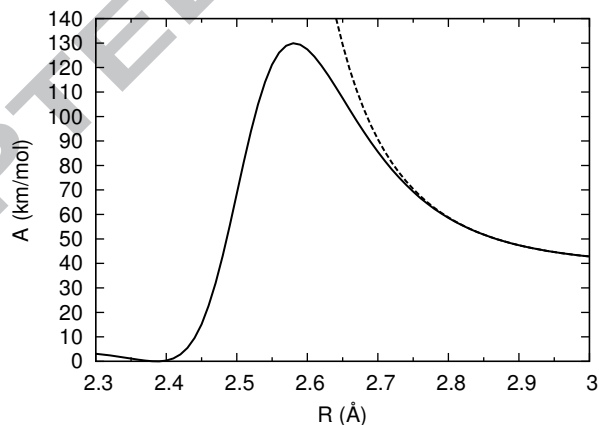
Figure 7: Dependence of the intensity of the $1^- \leftarrow 0^+$ transition on R. For this transition, the intensity for weak H-bonds ($R \sim 2.7$ to 3.0 Å) is the same as that of the fundamental ($1^+ \leftarrow 0^-$) (shown as the dashed curve) since the tunnel-split ground and excited states are hardly distinct (compare Figure 1). It is only for stronger H-bonds that this transition may be considered distinct from the fundamental.
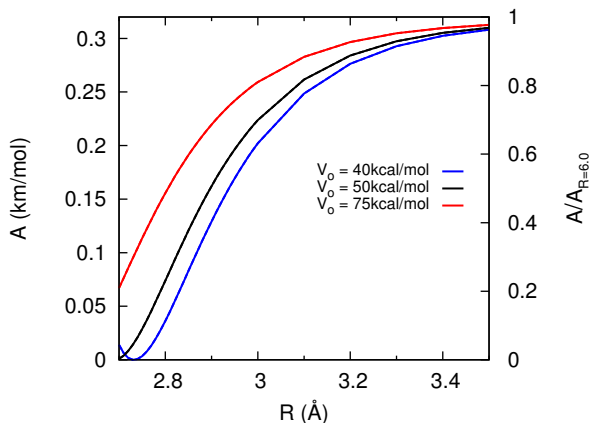
31

Figure 8: Intensity of the $2^+ \leftarrow 0^-$ overtone transition for different asymmetries, viz. $V_o = 40$, 50, and 75 kcal/mol. These plots contrast to the symmetric case (inset of Figure 6), showing that the extent and donor-acceptor distance range of overtone suppression in an H-bond (relative to a free OH) changes when the double-well potential is asymmetric. The plots also show that these properties can vary with the amount of asymmetry (V_o).
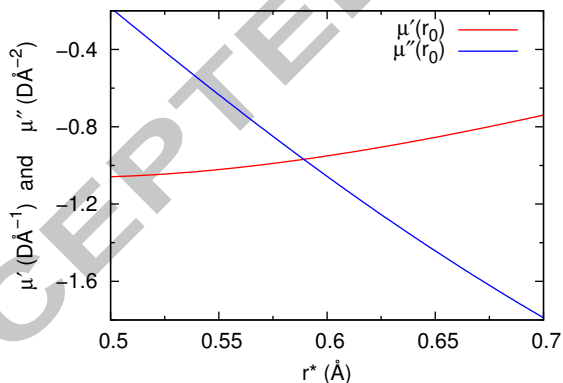

Figure 9: Parameter sensitivity of the dipole derivatives. First and second derivatives of the Mecke function, $\mu_0(r) = \mu^* r \exp(-r/r^*)$, evaluated at $r = r_0 = 0.96$ Å for a range of r^* values. The OH bond r^* value of 0.6 Å, given by Lawton and Child [50], has been used in all earlier plots in this work. The first and second derivatives are relevant to the intensity of the fundamental and overtone transitions, respectively. Note that the first derivative varies little for the parameter range shown whereas the second derivative varies by a factor of about five.
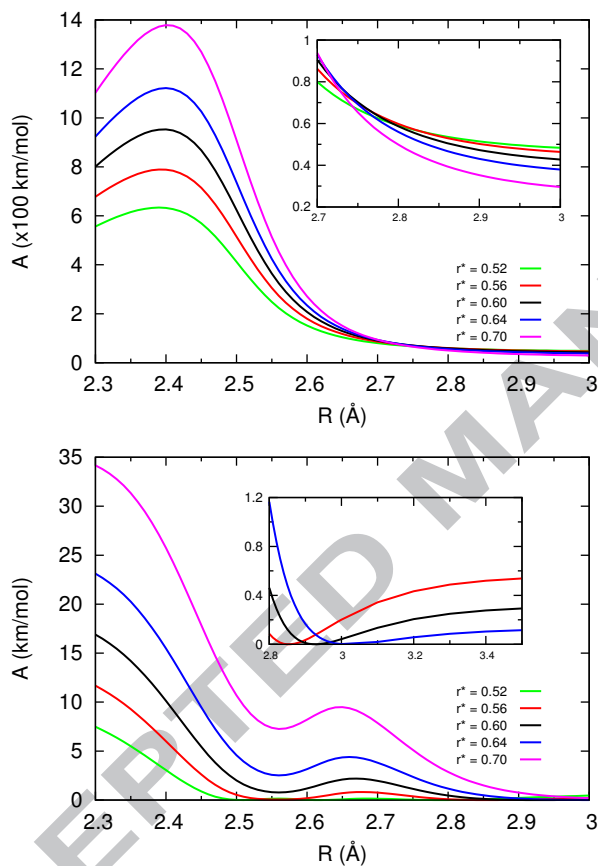
32

Figure 10: Variation of fundamental (left panel) and overtone (right panel) intensity with R for different Mecke parameters r^*. The $r^* = 0.6$ Å curves are both the same as those in Figures 2 and 6. The left panel shows that the fundamental enhancement is only somewhat affected by r^*, especially for weak bonds, while the overtone intensities change more dramatically. The fundamental intensities show a curious trend switch around 2.75 Å, which is shown in the inset and analysed in the main text.
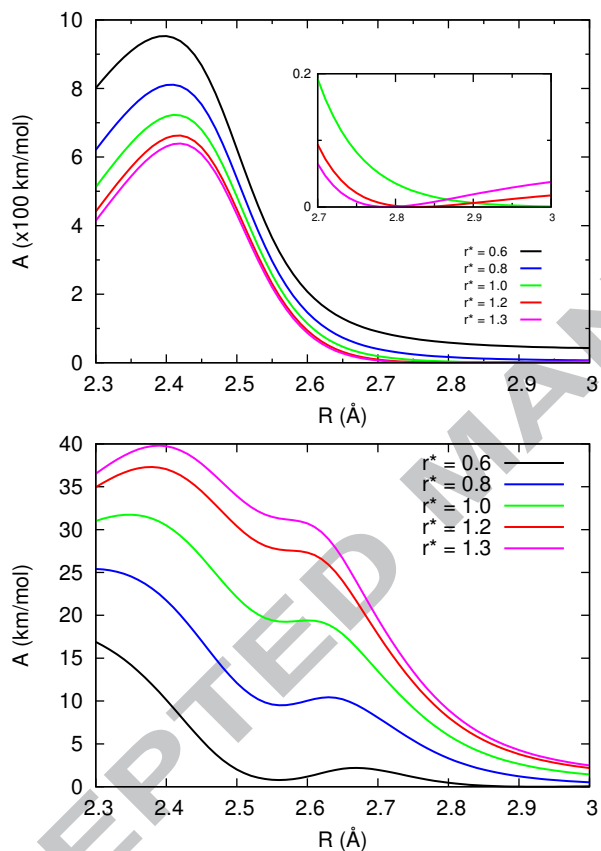
Figure 11: Plots of fundamental (left panel) and overtone (right panel) for the Mecke parameter r^* ranging from 0.6 to 1.3 Å. For each r^*, the μ^* value is also changed using the constraint that the Mecke function value at the reference distance of $r_0 = 0.96$ Å remains unchanged. The plots show that the fundamental and overtone are both enhanced at short R for all the r^* values used. However, for $r^* > r_0$, the fundamental is suppressed for weak H-bonds(inset). No suppression in this region is evident for the overtone.

34